Study on Anti-loosening Performance of D-shaped Bolt of Aero-engine

Qingyuan Lin, Bin Yang, Lintao Wang, Xianlian Zhang, Wei Sun, Qingchao Sun*

School of Mechanical Engineering, Dalian University of Technology, Dalian 116024, China

Abstract: Bolt connection has the advantages of simple connection, compact connection and easy assembly and disassembly. It is widely used in aero-engine connection structure. In this paper, non-standard connection bolt of low pressure turbo shaft disk of aero-engine is studied. The change rule of bolt tension in service was studied. Firstly, the stress of bolt underhead bearing and thread face under dynamic transverse load is analyzed. The function of bolt tension with time is obtained by calculating the friction moment. The anti-loosening performance data are obtained by transverse vibration test, and the validity of the theoretical model is verified. The effect of various system parameters on the anti-loosening performance of bolts is studied by using theoretical model. The theoretical model can effectively predict the anti-loosening performance of such bolts. The conclusion obtained in this paper can provide reference for the design and use of the connecting bolt of aero-engine.

Keywords: Aero-engine; Bolt tension; Anti-loosening performance

1 Introduction

Bolts are the basic parts of mechanical equipment. Bolt connection is a common fastening method, which has the advantages of simple use, compact structure and convenient assembly and disassembly. The quality of bolt connection structure will directly affect the overall performance of equipment. 70%~90% of the failure modes of mechanical equipment are directly related to the failure of bolt connection[1].

Aero-engine is a typical high speed, high pressure, high temperature and high reliability equipment, known as the pearl on the crown of manufacturing. Bolt connection is the main connection form of aero-engine. Assembly quality directly affects the performance of the engine and

* Corresponding author (qingchao@dlut.edu.cn)

 ISSN 2572-4975 (Print), 2572-4991 (Online)

largely determines the final quality, manufacturing cost and production cycle of the engine. Aero-engine assembly process is difficult and involves many disciplines, which is one of the key bottlenecks restricting the engine manufacturing level. Many researches have been carried out on the assembly performance test, prediction and control technology of aero-engine. However, most of the researches focus on the static initial characteristics of the connection structure, and few researches focus on the evolution of the connection state during the service of aero-engine.

Scholars have done a lot of research and analysis on the evolution of bolt tension. Schmitt[2] and Ibrahim[3] found in their study that the screw contact surface would suffer from fretting wear when the bolt was subjected to axial loading. In this case, the bolt tension would decline. When the bolt tension fell to the point where the thread self-locking could not be satisfied, the bolt and nut would move relatively and the bolt tension would decline. Sakai[4] divides the loosening process into two stages according to the relative motion of the screw pair: in the first stage, the relative motion of the screw pair is very small, and there is fretting wear between the thread contact surfaces; in the second stage, the screw pair has obvious relative motion. Junker[5] invented Junker transverse vibration testing machine, which is still widely used today. Junker analyzed the force on the threaded bevel and found that after the lateral dynamic load destroyed the friction constraint of the threaded pair, the component forces along the bevel direction would push the bolt to rotate and loosen. Based on this, the slope-slider model was established to explain why the dynamic load would reduce the anti-loosening performance of the bolt connection. Since then, researchers[6-10] have used Junker vibration testing machine to conduct extensive research on the looseness characteristics of bolt connections. However, there is still no general loosening model for all kinds of bolts and nuts.

Based on aero-engine low pressure turbine shaft disc connection bolts as the research object, to establish theoretical model of it, the anti-loosening performance were predicted and compared with the test result and provide reference for the improvement of the assembly performance of the aero-engine.

2 Mechanical analysis of connection bolt of low pressure turbine shaft disc

2.1 Stress analysis of bolt

Non-standard bolts are used in the low pressure turbine shaft disc of the aero-engine. As shown in Fig. 1, the bolt underhead bearing is a ’D’-shaped plane. The bolts described below are of such type.

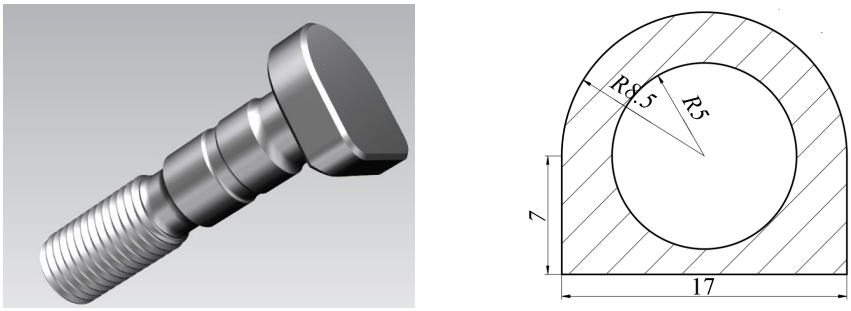

[A]: Schematic of bolt [B]: Dimensional drawing of the underhead bearing

Fig. 1 Bolt with 'D'-shaped underhead bearing

Friction is always opposite to the relative velocity vector on the underhead bearing. As shown in Fig. 2, the relative velocity $\mathbf{V}_a$ of the node on the underhead bearing is composed of the translation velocity $\mathbf{V}_1$ caused by the transverse load and the velocity $\mathbf{V}_2$ caused by the relative rotation. The lateral motion is in the x direction. The relative translation velocity $\mathbf{V}_1$ is going in the x direction. The relative velocity $\mathbf{V}_2$ is perpendicular to the position vector r.

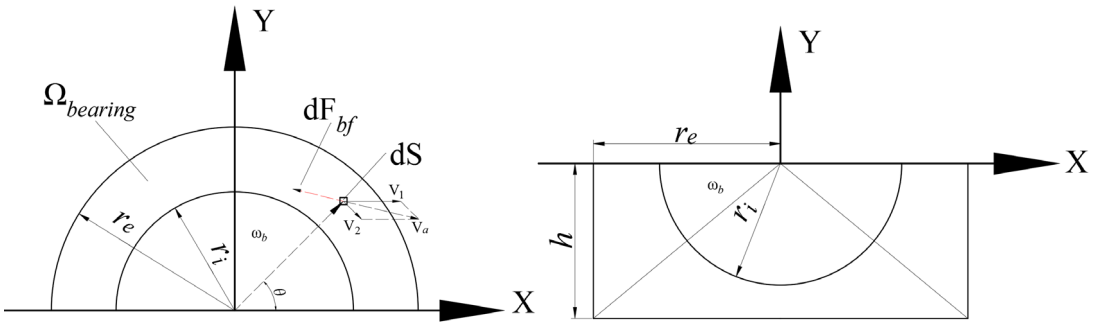

Fig. 2 The relative movement on the underhead bearing with respect to the joint members

$$\mathbf{v}_a = \mathbf{v}_1 + \mathbf{v}_2 = v_{b1}\mathbf{i} + \left(\omega_b \mathbf{k}\right) \times \mathbf{r} = \left(v_{b1} + \omega_b r \sin\theta\right)\mathbf{i} - \omega_b r \cos\theta \mathbf{j} \tag{1}$$

where dF_{bf} is the tangential friction force on the micro-element, r_i and r_e are the internal and external contact radius under bolt head, v_{bl} is the relative velocity of the bolt underhead bearing to the joint member area of contact surface along the x-axis, ω_b is the relative rotation angular velocity of the bolt underhead bearing to the joint, r is the radius direction of the point on the spherical surface, θ is the angle in the polar coordinate system, **i** is the unit vector along the x-axis, **j** is the unit vector along the y-axis direction and **k** is the unit vector along the z-axis.

Considering the bending effect of bolts under transverse load, it is assumed that the bolt pressure distribution is

$$q_b = q_{b0} + q_b^{'} \frac{x}{r_e} \tag{2}$$

 ISSN 2572-4975 (Print), 2572-4991 (Online)

where q_b is the underhead bearing pressure, q_{b0} is the average pressure on the contact bearing surface and $q_b^{'}$ is the pressure variation amplitude.

The direction of the friction force dF_{bf} is opposite to the direction of relative movement or movement tendency

$$d\mathbf{F}_{bf} = -dF_{bf}\frac{\mathbf{v}_a}{v_a} = -\frac{\left(v_{b1}+\omega_b y\right)\mathbf{i}-\omega_b x\mathbf{j}}{\sqrt{\left(v_{b1}+\omega_b y\right)^2+\left(\omega_b x\right)^2}}dF_{bf} \tag{3}$$

Based on Coulomb friction condition, we have

$$dF_{bf} = \mu_b q dS = \mu_b\left(q_{b0}+q_b^{'}\frac{r\cos\theta}{r_e}\right)dS \tag{4}$$

where μ_b is the underhead bearing friction coefficient.

The underhead bearing friction torque dT_b caused by the friction force dF_{bf} is

$$\begin{aligned} d\mathbf{T}_b &= \mathbf{r}\times d\mathbf{F}_{bf} = -(r\cos\theta\mathbf{i}+r\sin\theta\mathbf{j})\times\frac{\left(v_{b1}+\omega_b r\sin\theta\right)\mathbf{i}-\omega_b r\cos\theta\mathbf{j}}{\sqrt{\left(v_{b1}+\omega_b r\sin\theta\right)^2+\left(\omega_b r\cos\theta\right)^2}}dF_{bf} \\ &= dF_{bf}\frac{\omega_b r^2+v_{b1}r\sin\theta}{\sqrt{v_{b1}^2+2\omega_b v_{b1}\sin\theta+\omega_b^2 r^2}}\mathbf{k} \end{aligned} \tag{5}$$

The underhead bearing friction torque T_b can be presented by integrating dT_b on the contact bearing area.

$$\begin{aligned} T_b &= \iint_{\Omega_{\text{bearing}}} dT_b \\ &= \iint_{\Omega_{\text{bearing}}} \mu_b\left(q_{b0}+q_b^{'}\frac{r\cos\theta}{r_e}\right)\times\frac{\omega_b r^2+v_{b1}r\sin\theta}{\sqrt{v_{b1}^2+2\omega_b v_{b1}\sin\theta+\omega_b^2 r^2}}dS \\ &= \mu_b q_{b0}\left(\int_{r_i}^{r_e} r^2 dr\int_0^{\pi}\frac{\left(\eta_b+r\sin\theta\right)d\theta}{\sqrt{\eta_b^2+r^2+2\eta_b r\sin\theta}}+\int_{r_i}^{-r_e/\cos\theta} r^2 dr\int_{\pi}^{\pi+\arctan\frac{h}{r_e}}\frac{\left(\eta_b+r\sin\theta\right)d\theta}{\sqrt{\eta_b^2+r^2+2\eta_b r\sin\theta}}+\right. \\ &\left.\int_{r_i}^{-h/\sin\theta} r^2 dr\int_{\pi+\arctan\frac{h}{r_e}}^{2\pi-\arctan\frac{h}{r_e}}\frac{\left(\eta_b+r\sin\theta\right)d\theta}{\sqrt{\eta_b^2+r^2+2\eta_b r\sin\theta}}+\int_{r_i}^{r_e/\cos\theta} r^2 dr\int_{2\pi-\arctan\frac{h}{r_e}}^{2\pi}\frac{\left(\eta_b+r\sin\theta\right)d\theta}{\sqrt{\eta_b^2+r^2+2\eta_b r\sin\theta}}\right) \\ &+\frac{\mu_b q_b^{'}}{r_e}\left(\int_{r_i}^{r_e} r^3 dr\int_0^{\pi}\frac{\left(\eta_b+r\sin\theta\right)\cos\theta d\theta}{\sqrt{\eta_b^2+r^2+2\eta_b r\sin\theta}}+\int_{r_i}^{-r_e/\cos\theta} r^3 dr\int_{\pi}^{\pi+\arctan\frac{h}{r_e}}\frac{\left(\eta_b+r\sin\theta\right)\cos\theta d\theta}{\sqrt{\eta_b^2+r^2+2\eta_b r\sin\theta}}+\right. \\ &\left.\int_{r_i}^{-h/\sin\theta} r^3 dr\int_{\pi+\arctan\frac{h}{r_e}}^{2\pi-\arctan\frac{h}{r_e}}\frac{\left(\eta_b+r\sin\theta\right)\cos\theta d\theta}{\sqrt{\eta_b^2+r^2+2\eta_b r\sin\theta}}+\int_{r_i}^{r_e/\cos\theta} r^3 dr\int_{2\pi-\arctan\frac{h}{r_e}}^{2\pi}\frac{\left(\eta_b+r\sin\theta\right)\cos\theta d\theta}{\sqrt{\eta_b^2+r^2+2\eta_b r\sin\theta}}\right) \end{aligned} \tag{6}$$

where $\eta_b = v_{bl} / \omega_b$ is the bearing translation-rotational ratio.

T_b and F_{bs} can be presented as the functions of η_b as follows:

$$\begin{aligned} R_{Tb} &= \left| \frac{T_b}{\mu_b q_{b0}} \right| \\ &= \int_{r_i}^{r_e} r^2 dr \int_0^{\pi} \frac{(\eta_b \sin\theta + r) d\theta}{\sqrt{\eta_b^2 + r^2 + 2\eta_b r \sin\theta}} + \int_{r_i}^{-r_e/\cos\theta} r^2 dr \int_{\pi}^{\pi + \arctan\frac{h}{r_e}} \frac{(\eta_b \sin\theta + r) d\theta}{\sqrt{\eta_b^2 + r^2 + 2\eta_b r \sin\theta}} + \\ &\int_{r_i}^{-h/\sin\theta} r^2 dr \int_{\pi + \arctan\frac{h}{r_e}}^{2\pi - \arctan\frac{h}{r_e}} \frac{(\eta_b \sin\theta + r) d\theta}{\sqrt{\eta_b^2 + r^2 + 2\eta_b r \sin\theta}} + \int_{r_i}^{r_e/\cos\theta} r^2 dr \int_{2\pi - \arctan\frac{h}{r_e}}^{2\pi} \frac{(\eta_b \sin\theta + r) d\theta}{\sqrt{\eta_b^2 + r^2 + 2\eta_b r \sin\theta}} \end{aligned} \tag{7}$$

$$\begin{aligned} R_{Fb} &= \left| \frac{F_{bs}}{\mu_b q_{b0}} \right| \\ &= \int_{r_i}^{r_e} r dr \int_0^{\pi} \frac{(\eta_b + r \sin\theta) d\theta}{\sqrt{\eta_b^2 + r^2 + 2\eta_b r \sin\theta}} + \int_{r_i}^{-r_e/\cos\theta} r dr \int_{\pi}^{\pi + \arctan\frac{h}{r_e}} \frac{(\eta_b + r \sin\theta) d\theta}{\sqrt{\eta_b^2 + r^2 + 2\eta_b r \sin\theta}} + \\ &\int_{r_i}^{-h/\sin\theta} r dr \int_{\pi + \arctan\frac{h}{r_e}}^{2\pi - \arctan\frac{h}{r_e}} \frac{(\eta_b + r \sin\theta) d\theta}{\sqrt{\eta_b^2 + r^2 + 2\eta_b r \sin\theta}} + \int_{r_i}^{r_e/\cos\theta} r dr \int_{2\pi - \arctan\frac{h}{r_e}}^{2\pi} \frac{(\eta_b + r \sin\theta) d\theta}{\sqrt{\eta_b^2 + r^2 + 2\eta_b r \sin\theta}} \end{aligned} \tag{8}$$

The numerical calculation methods of the thread friction torque T_t is given as follows[11]

$$R_{Tt} = \left| \frac{T_t}{\mu_t q_{t0}} \right| = \sqrt{\sec^2\alpha + \tan^2\beta} \times \int_{r_{\min}}^{r_{\max}} r^2 dr \int_0^{2\pi} \frac{(r - \eta_t \sin\theta) d\theta}{\sqrt{\eta_t^2 \left(1 + \tan^2\alpha \cos^2\theta\right) + r^2 - 2\eta_t r \sin\theta}} \tag{9}$$

$$R_{Ft} = \left| \frac{F_{ts}}{\mu_t q_{t0}} \right| = \sqrt{\sec^2\alpha + \tan^2\beta} \times \int_{r_{\min}}^{r_{\max}} r dr \int_0^{2\pi} \frac{(\eta_t - r \sin\theta) d\theta}{\sqrt{\eta_t^2 \left(1 + \tan^2\alpha \cos^2\theta\right) + r^2 - 2\eta_t r \sin\theta}} \tag{10}$$

where F_{ts} is the thread friction shear force, μ_t is the thread friction coefficient, q_{t0} is the average pressure on the contact thread surface, r_{min} and r_{maj} are the minor thread radius and the major thread radius, α is the half of thread profile angle, β is the lead helix angle, $\eta_t = v_{tx} / \omega_t$ is the thread translation-rotational ratio, R_{Tt} and R_{Ft} are the result of the numerical integration with respect to η_t.

2.2 Calculation of stiffness of connecting structure

We all know that stiffness and flexibility are reciprocal, so we get stiffness by calculating

 ISSN 2572-4975 (Print), 2572-4991 (Online)

flexibility.

The calculation formula of bolt flexibility δ_S is given by:

$$\delta_S = \frac{4}{\pi \cdot E_S}\left(\frac{0.5d}{d^2} + \frac{l_1}{d_T^2} + \frac{l_{Gew} + 0.5d}{d_3^2} + \frac{0.4d}{d^2}\right) \tag{11}$$

Where E_s is the Young's modulus of bolt material, d is the nominal diameter of bolt, dT is the diameter of bolt rod, d_3 is the

minor diameter of bolt, l_1 is the length of bolt rod and l_{Gew} is the loadable thread length of bolt.

And the bolt stiffness k_b is given by:

$$k_b = \frac{1}{\delta_S} \tag{12}$$

For stiffness of clamped part, firstly, take the auxiliary size value:

$$D_A = \left(\frac{2\pi PCD}{N_{blot}} - d_h + d_{fl}\right)/2 \tag{13}$$

$$\beta_L = l_k / d_{wa}, y = D'_A / d_{wa} \tag{14}$$

where D_A is the equivalent replacement of the outer diameter of the connecting part on the connecting interface, if the interface area is not circular, we should use average diameter (outer diameter of plane of nut support), PCD is the diameter node circle of the bolt center, d_h is bolt hole diameter, b_{fl} is flange width, N_{blot} is the number of bolts, β_L is the length ratio, y is the bending Angle of clamped part, l_k is the clamping length and d_{wa} is the outer diameter of the washer bearing surface in contact with the clamping part.

For the bolt group of low-pressure turbowheel shaft disc flange bolt, the bolt connection type is DSV, and the formula is as follows:

$$\tan\varphi_D = 0.362 + 0.032\ln(\beta_L / 2) + 0.153\ln y \tag{15}$$

where φ_D is the Angle of the replacement deformation cone of the bolt connection.

For the bolt connection type is DSV, we can obtain the maximum limiting outside diameter $D_{A,Gr}$:

$$D_{A,Gr} = d_{wa} + w \cdot l_k \cdot \tan\varphi_D \tag{16}$$

The flexibility of clamped part δ_P is given by:

$$\delta_P = \frac{2\ln\left[\frac{(d_{wa} + d_h)(d_{wa} + w \cdot l_k \cdot \tan\varphi_D - d_h)}{(d_{wa} - d_h)(d_{wa} + w \cdot l_k \cdot \tan\varphi_D + d_h)}\right]}{E_p \cdot \pi \cdot w \cdot d_h \cdot \tan\varphi_D} \tag{17}$$

And the stiffness of clamped part k_c is given by:

$$k_C = \frac{1}{\delta_P} \tag{18}$$

3 Mathematical model of bolt looseness

3.1 Load analysis of bolts

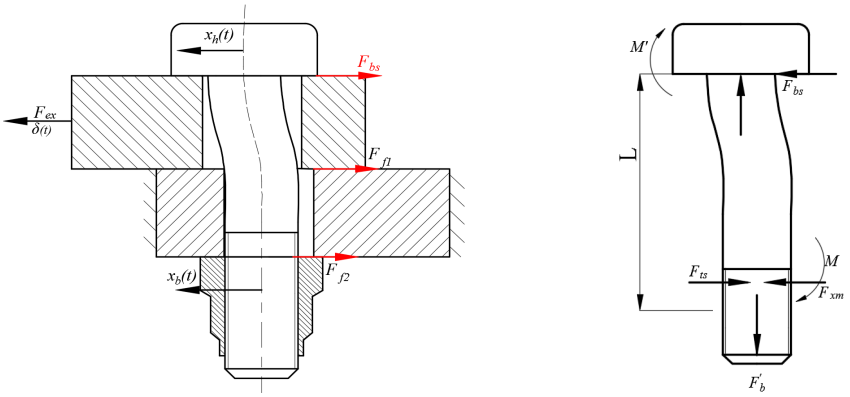

[A]: Schematic of connecting structure under load [B]: Load analysis of bolts

Fig. 3 Load analysis

If the transverse load on the bolt connection is small enough, the bolt head will move with the connected piece without relative movement, which is the basis of this study. At this time, the bolt deflection at the bolt head is expressed as follows:

$$\left|x_h(t) - x_t(t)\right| = \left|x_h(t)\right| = \left|\delta(t)\right| = \frac{kF_{bs}L^3}{3EI} \tag{19}$$

where k is the bending factor.

$$k = 1 - 3\lambda L / [4\lambda L + 16EIr_e / \pi\left(r_e^4 - r_i^4\right)] \tag{20}$$

where E is Young's elastic modulus, I is the axial moment of inertia for the cross sectional area, L is the effective bolt bending length and λ is a constant, which is dependent on the bolt underhead bending stiffness.

The deflection of bolt δ_J is equal to the transverse displacement load.

$$\delta_J = \delta_0 \sin\left(\omega' t\right) \tag{21}$$

 ISSN 2572-4975 (Print), 2572-4991 (Online)

Where δ_0 is the transverse displacement amplitude and ω' is the angular velocity for the excitation.

$$F_{bs} = \frac{3EI}{kL^3}\delta_0 \sin\left(\omega' t\right) \tag{22}$$

The thread friction shear force F_{ts} of bolt along the x-direction is given by[11]

$$F_{ts} = \frac{3EI}{kL^3}\delta_0 \sin\left(\omega' t\right)\left[1+\frac{\tan\alpha L}{\frac{r_{\min}\left(\gamma^4-1\right)}{2\left(\gamma^3-1\right)}+\left(\frac{1}{3}r_{\text{maj}}+0.2725p\right)}\times\frac{\frac{8EIr_e}{\pi\left(r_e^4-r_i^4\right)}+\lambda L}{\frac{8EIr_e}{\pi\left(r_e^4-r_i^4\right)}+2\lambda L}\right] \tag{23}$$

where $\tau = r_{maj}/r_{min}$.

3.2 Quantitative evolution model of bolt tension

As shown in FIG. 4, after the initial tightening stage, the bolt receives three torques T_b、T_t and T_p acting together around its axis.

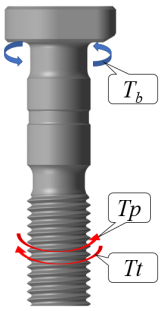

Fig. 4 A free body diagram of the bolt

When the bolt is not under load, the three torques are balanced. When the load reaches a certain level, the balance of the three torques is broken and the bolt turns. The bolt rotation angular acceleration $\dot{\omega}$ is given by

$$J\dot{\omega} = \left(T_p - T_{\text{bc}}' - T_{\text{tc}}'\right) \tag{24}$$

where J is the moment of the inertia of the bolt.

The calculation method of the bolt rotation angular velocity ω is given by

$$\omega = \omega_0 + \int_t^{t+\Delta t}\dot{\omega}dt \tag{25}$$

where ω_0 is the rotation angular velocity at time t.

The calculation method of $\Delta\theta'$ is given by

$$\Delta\theta' = \Delta\theta_0' + \int_0^{\Delta t} \omega dt \tag{26}$$

where $\Delta\theta_0'$ is the self-loosening angle at time 0.

The clamp force loss ΔF caused by the loosening rotation $\Delta\theta'$ is given by

$$\Delta F = \frac{k_b k_c}{k_b + k_c} \frac{\Delta\theta'}{2\pi} \cdot P \tag{27}$$

where P is the thread pitch.

4 Experiment

4.1 Experiment environment

According to Junker transverse vibration testing machine, this study designed and built a bolt transverse vibration test bed.

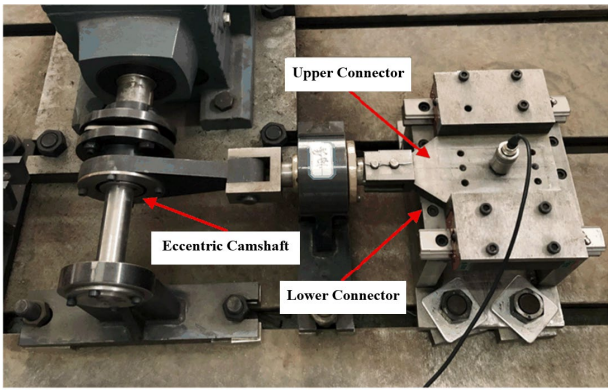

Fig. 5 Bolt transverse vibration test bed

As shown in Fig. 5, the bolt transverse vibration test bed is driven by three asynchronous motors. The motor is connected to the external crank slider mechanism by eccentric camshaft, and the crank slider mechanism is connected to the upper connector at the threaded joint by elastomer and transverse force sensor. The lower connector at the threaded joint is fixed on the horizontal table, and lubricating oil is used between the upper and lower connectors. The motor drives the camshaft to move, generating transverse sinusoidal displacement excitation. By controlling the rotation speed of three asynchronous motors and adjusting the eccentricity of eccentric camshaft, the frequency and

 ISSN 2572-4975 (Print), 2572-4991 (Online)

amplitude of transverse displacement of sine wave can be controlled.

Tighten the bolts before the test to generate the initial preload on the upper and lower connectors. The change of bolt tension in the test can be measured by the pressure sensor between the nut and the lower connector, the measurement of lateral displacement of the upper connector can be completed by the eddy current sensor behind the test bench, and the change of lateral force in the test can be measured by the lateral force sensor.

4.2 Experiment result

Bolts were tested under the four kinds of initial preloading forces of 12000*N* 20000*N* 30000*N* and 33000*N* respectively. The transverse load frequency was 4*HZ* and the amplitude was 0.2*mm*, which is much smaller than the unilateral hole clearance between the bolt and the hole in connector. Young's modulus and Poisson's ratio of connecting parts used in the test were 200*GPA* and 0.3 respectively. The test results are shown in Fig. 6.

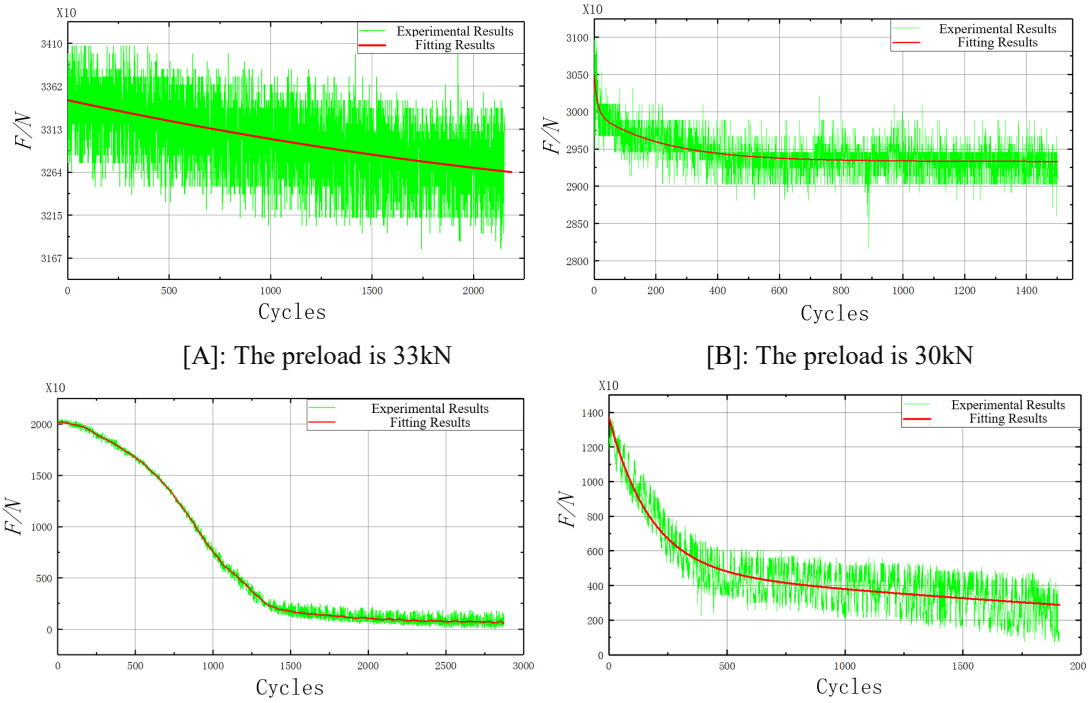

[A]: The preload is 33kN

[B]: The preload is 30kN

[C]: The preload is 20kN

[D]: The preload is 12kN

Fig. 6 Experimental curve for bolt tension

In order to verify the correctness of the theoretical calculation method, the changes of bolt tension under the three kinds of initial preloading forces of 30*kN*, 20*kN* and 12*kN* obtained from the

test are compared with the results obtained from the theoretical calculation. The theoretical calculation results are consistent with the experimental results.

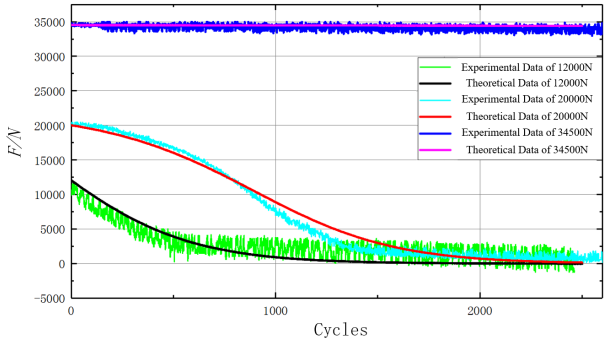

Fig. 7 The comparison between theoretical data and experimental data

As shown in Fig. 7, in the case of initial preloading force of 34500*N*, with the continuous application of load, *F* remains unchanged. This is because the transverse load did not reach the minimum value that would cause the bolt to loosen. When the initial preloading force is set at 20000*N*, *F* decreases. When the initial preloading force drops to 12000*N*, *F* decreases rapidly. The experimental results verify the accuracy of the theoretical calculation method.

5 Influence of system parameters on bolt anti-loosening performance

According to the theoretical calculation method, the influence of underhead bearing friction coefficient μ_b, thread friction coefficient μ_t, initial preload of bolt F_0 and transverse load δ_0 on bolt release performance are calculated respectively.

When F_0 is 20*kN*, δ_0 is 0.07mm and μ_t is 0.2, μ_b is discretized between 0.1 to 0.2. As shown in Fig. 8, the smaller μ_b, the faster the bolt will become loose.

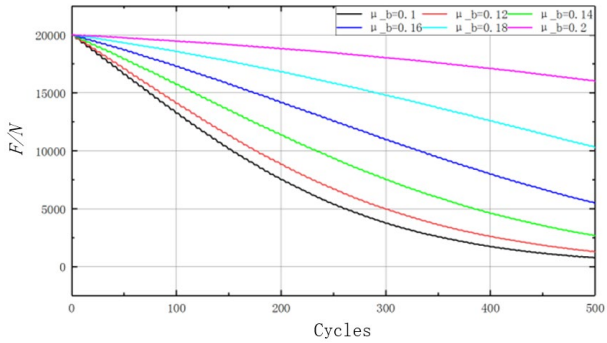

Fig. 8 Influence curve of friction of μ_b on bolt anti - loosening performance

 ISSN 2572-4975 (Print), 2572-4991 (Online)

When F_0 is 20kN, δ_0 is 0.07mm and μ_b is 0.2, μ_t is discretized between 0.1 to 0.2. As shown in Fig. 9, the smaller μ_t, the faster the bolt will become loose. At the same time, μ_b has a greater influence on bolt loosening performance than μ_t.

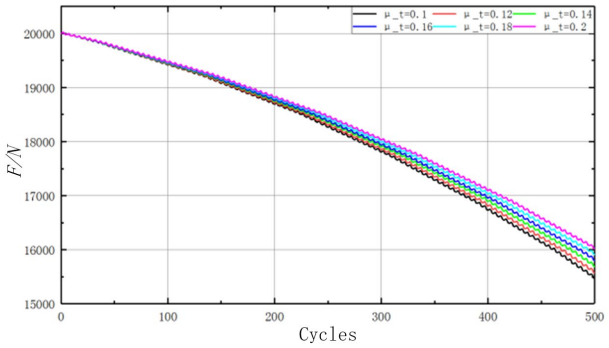

Fig. 9 Influence curve of friction of μt on bolt anti - loosening performance

When δ_0 is 0.07mm, μ_t is 0.2 and μ_b is 0.2, F_0 is discretized between 10kN to 35kN. The final result is normalized. As shown in Fig. 10, the smaller F_0, the faster the bolt will become loose.

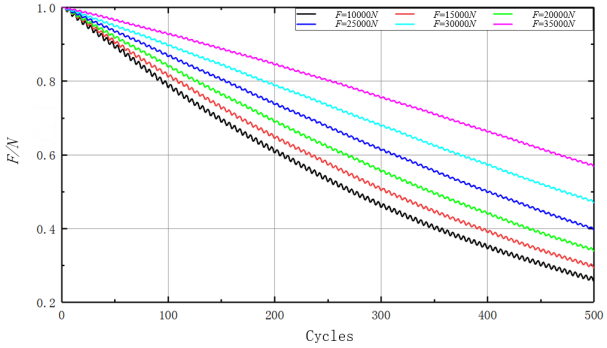

Fig. 10 Influence curve of friction of F_0 on bolt anti - loosening performance

When F_0 is 20kN, μ_t is 0.2 and μ_b is 0.2, δ_0 is discretized between 0.05mm to 0.1mm. The final result is normalized. As shown in Fig. 11, the bigger δ_0, the faster the bolt will become loose. It is also found that there is a load critical value. Below this critical value, the bolt will not become loose.

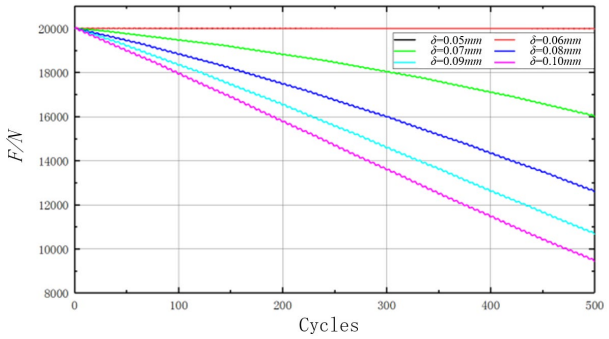

Fig. 11 Influence curve of friction of δ_0 on bolt anti - loosening performance

6 Conclusion

In this paper, the anti-loosening performance of 'D'-shaped bolt of aero-engine low pressure turbine shaft disc is studied theoretically and experimentally. The theoretical calculation and experimental results denote the following:

1. The evolution model of bolt tension for 'D'-shaped bolt is established, which takes into account the structural parameters, load, initial preload and other parameters of the connecting system, and can predict the change trend of bolt tension under the service.

2. Through the transverse vibration test of the connecting structure, the anti-loosening performance of 'D'-shaped bolt are obtained, which is consistent with the theoretical calculation results and verifies the accuracy of the evolution model of bolt tension.

3. Through the analysis of different structural parameters, the action mode and influence degree of each parameter on the anti-loosening performance of 'D'-shaped bolt are obtained.

The experimental results show that the bolt tension evolution model established in this paper is effective and can be used to predict the anti-loosening performance of 'D'-shaped bolts under different system parameters. The research results in this paper can provide reference for the design and use of 'D'-shaped bolt of aero-engine low pressure turbine shaft disc.

Acknowledgements

This work was supported by LiaoNing Revitalization Talents Program [XLYC1808016], and the Fundamental Research Funds for the Central Universities of China [DUT18LAB04,DUT19LAB17].

References

[1] Wang B Q , Chen L R, Chen X F, High-strength bolted connection,1991.1.

[2] Izumi S, Yokoyama T, Kimura M, et al. Loosening-resistance evaluation of double-nut tightening method and spring washer by three-dimensional finite element analysis, ***Engineering Failure Analysis,*** 2009, 16(5):1510-1519.

[3] Yokoyama T, Izumi S, Sakai S, analytical modeling of the transverse load-displacement relation of a bolted joint with consideration of the mechanical behavior on contact surfaces, ***ASME 2009 Pressure Vessels and Piping Conference***, 2009:477-486.

[4] Sakai T, Investigations of bolt loosening mechanisms : 1st report, on the bolts of transversely loaded joints, ***Bulletin of Jsme,*** 1978, 21(377):279-287.

[5] Junker G H, Criteria for self loosening of fasteners under vibration. ***Aircraft Engineering & Aerospace Technology,*** 1969, 44(10):14-16.

[6] Nassar Sayed A, Matin Payam H, Clamp load loss due to fastener elongation beyond its elastic limit, ***Journal of Pressure Vessel Technology-transactions of the ASME***,2006;128(3): p.379-387.

[7] Nassar S A, Yang X J, et al. Nonlinear deformation behavior of clamped bolted joints under a separating service load, ***Journal of Pressure Vessel Technology-transactions of the ASME***,2011;133(2).

[8] Yang X J, Nassar S A, et al. Clamp load loss in a bolted joint model with plastic bolt elongation and eccentric service load, ***Proceedings of the ASME Pressure Vessels and Piping Conference,***2010; p.139-149.

[9] Yang X J, Nassar S A, et al. Nonlinear Behavior of preloaded bolted joints under a cyclic separating load, ***Journal of Pressure Vessel Technology-transactions of the ASME***,2012;134(1).

[10] Benhaddou T, Stephan P, Daidie A, et al. Effect of axial preload on durability of aerospace fastened joints, ***International Journal of Mechanical Sciences,*** 2018;137: p.214-223.

[11] Nassar S A, Yang X J, A mathematical model for vibration-induced loosening of preloaded threaded fasteners, ***Journal of Vibration and Acoustics-transactions of the ASME,***2009;131(2).